MOLECULAR AND CELLULAR BIOLOGY, July 2010, p. 3329–3341 Vol. 30, No. 13
0270-7306/10/$12.00 doi:10.1128/MCB.01590-09

Thiamine Biosynthesis in *Saccharomyces cerevisiae* Is Regulated by the NAD^+-Dependent Histone Deacetylase Hst1▽†

Mingguang Li,[1] Brian J. Petteys,[2] Julie M. McClure,[1] Veena Valsakumar,[1] Stefan Bekiranov,[1] Elizabeth L. Frank,[3] and Jeffrey S. Smith[1]*

Department of Biochemistry and Molecular Genetics, University of Virginia Health System, School of Medicine, Charlottesville, Virginia 22908[1]; ARUP Laboratories, 500 Chipeta Way, Salt Lake City, Utah 84108[2]; and Department of Pathology, University of Utah Health Sciences Center, Salt Lake City, Utah 84112[3]

Received 10 December 2009/Returned for modification 4 January 2010/Accepted 21 April 2010

Genes encoding thiamine biosynthesis enzymes in microorganisms are tightly regulated such that low environmental thiamine concentrations activate transcription and high concentrations are repressive. We have determined that multiple thiamine (*THI*) genes in *Saccharomyces cerevisiae* are also regulated by the intracellular NAD^+ concentration via the NAD^+-dependent histone deacetylase (HDAC) Hst1 and, to a lesser extent, Sir2. Both of these HDACs associate with a distal region of the affected *THI* gene promoters that does not overlap with a previously defined enhancer region bound by the thiamine-responsive Thi2/Thi3/Pdc2 transcriptional activators. The specificity of histone H3 and/or H4 deacetylation carried out by Hst1 and Sir2 at the distal promoter region depends on the *THI* gene being tested. Hst1/Sir2-mediated repression of the *THI* genes occurs at the level of basal expression, thus representing the first set of transcription factors shown to actively repress this gene class. Importantly, lowering the NAD^+ concentration and inhibiting the Hst1/Sum1 HDAC complex elevated the intracellular thiamine concentration due to increased thiamine biosynthesis and transport, implicating NAD^+ in the control of thiamine homeostasis.

Vitamin B1 (thiamine) in the form of thiamine pyrophosphate (TPP) is an essential cofactor for enzymes that decarboxylate α-keto acids, including α-ketoglutarate dehydrogenase, branched-chain α-ketoacid dehydrogenase, and transketolase, during amino acid and carbohydrate metabolism. Animals are unable to synthesize thiamine and have to obtain it from their diet, whereas microorganisms such as bacteria and the budding yeast, *Saccharomyces cerevisiae*, encode pathways for synthesizing thiamine *de novo* and also import thiamine from the environment (22, 43). Dietary sources of thiamine include cereal grains, vegetables, and meats. Well-known human diseases caused by thiamine deficiency include beri-beri and Wernicke-Korsakoff syndrome.

Thiamine was the first water-soluble B-complex vitamin to be discovered, through its ability to reverse the effects of beriberi in animals (15). Its synthesis has been well characterized in bacteria, but knowledge of the early steps of *de novo* synthesis in yeast is less complete (25). Yeast first separately synthesizes two precursors, 5-(2-hydroxyethyl)-4-methylthiazole phosphate (HET-P) and 4-amino-5-hydroxymethyl-2-methylpyrimidine diphosphate (HMP-PP) through poorly understood mechanisms. These thiazole and pyrimidine substrates are ultimately condensed into thiamine monophosphate in a later step of the pathway. HMP-PP is synthesized in yeast cells from histidine and pyridoxal-5-phosphate (PLP; vitamin B6), thus providing a link between the synthesis pathways for these two soluble B vitamins. The substrates for HET-P synthesis include cysteine, glycine, and D-pentulose-5-phosphate (25). More recently, synthesis of the HET-P moiety was shown to also proceed through an advanced intermediate generated by the Thi4 protein in a reaction that consumes NAD^+ as a substrate, releasing nicotinamide (NAM) as a by-product (12). NAM and nicotinic acid (NA) are both considered forms of niacin (vitamin B3) and are precursors for NAD^+ biosynthesis via salvage pathways. Thi4, therefore, provides a direct link between thiamine biosynthesis and another B-complex vitamin. The expression of *THI4* and other thiamine biosynthesis genes is inversely regulated by the amount of thiamine available in the growth medium, with low thiamine inducing *THI* gene expression and high thiamine repressing *THI* gene expression (22). Up until now, a relationship between *THI* gene expression and NAD^+ biosynthesis had not been established.

In addition to its role as an electron acceptor in oxidoreductase reactions, NAD^+ is used as a cosubstrate by the sirtuin family of NAD^+-dependent protein deacetylases (23, 28). These enzymes consume NAD^+ as part of their reaction mechanism, in which the deacetylation of a target protein is coupled to cleavage of NAD^+, releasing NAM, 2′-*O*-acetyl ADP ribose, and the deacetylated protein as products (27, 52, 57). Yeast Sir2 functions in heterochromatic gene silencing at telomeres, the silent mating-type loci, and the ribosomal DNA (rDNA) locus (for a review, see reference 9). SIRT1 is the closest homolog to Sir2 in mammals and deacetylates numerous important regulatory proteins, including p53 and NF-κB (29, 38, 58, 61).

The consumption of NAD^+ by sirtuins results in a requirement for NAD^+ biosynthesis and salvage pathways to maintain sufficiently high NAD^+ concentrations in the various cellular compartments, including in the nucleus, to support histone/

* Corresponding author. Mailing address: Department of Biochemistry and Molecular Genetics, University of Virginia Health System, School of Medicine, Jordan Hall, Box 800733, Charlottesville, VA 22908. Phone: (434) 243-5964. Fax: (434) 924-5069. E-mail: jss5y@virginia.edu.

† Supplemental material for this article may be found at http://mcb.asm.org/.

▽ Published ahead of print on 3 May 2010.

protein deacetylation and heterochromatic gene silencing (1, 48, 51). NAD^+ is synthesized *de novo* in multiple enzymatic steps carried out by the Bna1-Bna6 proteins to synthesize nicotinic acid mononucleotide (NaMN) (26), which is then converted to NAD^+ by the adenylyltransferases Nma1 and Nma2 (1) and then NAD synthetase (Qns1) (6) (Fig. 1A). In yeast cells, NAD^+ that is broken down to NAM by sirtuins or other NAD^+-consuming enzymes is salvaged by conversion to nicotinic acid by the nicotinamidase Pnc1 (19), followed by conversion of NA to NaMN by the nicotinic acid phosphoribosyltransferase, Npt1, the rate-limiting step of the Preiss-Handler "NAD^+ salvage" pathway (47). In the absence of Npt1, the intracellular NAD^+ concentration is reduced by 2- to 3-fold, resulting in defects of Sir2-mediated silencing and replicative longevity (4, 32, 54). NAM is a strong sirtuin inhibitor (7, 27), and its accumulation in the absence of Pnc1 also results in silencing defects due to Sir2 inhibition (17).

The closest paralog of Sir2 in yeast cells is the Hst1 protein (8), and they have been shown to substitute for each other in silencing under specialized conditions (8, 21, 56). Hst1 is normally recruited to the promoters of specific middle sporulation and *de novo* NAD^+ biosynthesis genes with its binding partner Sum1, where it acts as a transcriptional corepressor (3, 60). Deletion of *NPT1* leads to inhibition of Hst1 and elevated expression of these target genes (3). The induction of *de novo* NAD^+ biosynthesis genes in the absence of Npt1 is likely a compensatory mechanism to maintain NAD^+ homeostasis (3). We were interested in comparing the effects on global gene expression caused by the deletion of *NPT1* or *PNC1* or the addition of 5 mM NAM to the growth medium. In the process, we discovered that the *de novo* thiamine biosynthesis genes are upregulated by these conditions and that they are normally repressed by histone deacetylation at their promoters mediated by Hst1 and, to a lesser extent, Sir2. The derepression of the thiamine genes results in increased accumulation of intracellular thiamine levels. Thiamine and NAD^+ homeostasis in yeast cells are therefore linked by regulation of the NAD^+-dependent histone deacetylase (HDAC) Hst1.

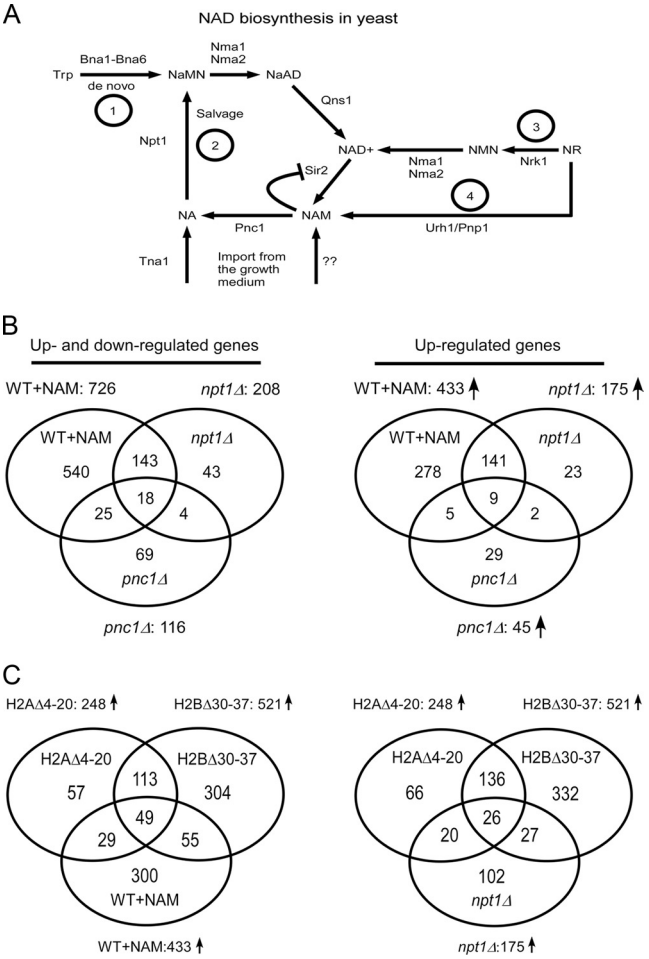

FIG. 1. Effects of elevated nicotinamide and reduced NAD^+ concentrations on global gene expression. (A) Schematic diagram of NAD^+ biosynthesis in yeast. NAD^+ can be synthesized by a *de novo* pathway starting with tryptophan (Trp) (1) or through the Preiss-Handler NAD^+ salvage pathway, where nicotinamide (NAM) produced by Sir2 or other sirtuins is deamidated by the nicotinamidase Pnc1 to form nicotinic acid (NA) (2). The nicotinic acid phosphoribosyl transferase Npt1 converts NA into nicotinic acid mononucleotide (NaMN). Alternatively, NA is imported from the growth medium by the nicotinic acid permease (Tna1). Nicotinamide riboside (NR) can be utilized as an NAD^+ precursor either by phosphorylation by the nicotinamide riboside kinase (Nrk1) to form nicotinamide mononucleotide (NMN) (3) or by degradation into NAM via Pnp1 (a phosphorylase) and Urh1 (a hydrolase) (4). Additional abbreviations: NaAD, deamido-NAD^+; Qns1, NAD synthetase; Nma1 and Nma2, nicotinate mononucleotide adenylyltransferases. The import mechanism for NAM is uncharacterized. (B) Venn diagrams indicating the overlaps in gene expression changes (both overall and upregulated) between the *npt1*Δ and *pnc1*Δ mutants and the WT strain treated with 5 mM NAM. The total number of changes for each strain is also indicated. (C) Venn diagrams showing overlaps in upregulated genes induced by the WT + NAM (left) condition or the *npt1*Δ mutation (right) compared to previously determined upregulated genes from mutants with small deletions in the N-terminal H3 or H4 tails (45, 46).

MATERIALS AND METHODS

Media and yeast strains. Yeast strains were grown in either yeast extract-peptone-dextrose (YPD) or synthetic complete (SC) medium containing 2% glucose as the carbon source (11). Where indicated below, the SC medium was prepared lacking nicotinic acid (51) or containing various concentrations of thiamine. All yeast growth was performed at 30°C. The strains used in this study were derived from the JB740 strain background previously used for rDNA silencing studies (53) and are all listed in Table S1 in the supplemental material. The *NPT1*, *PNC1*, *BNA1*, *TNA1*, *SIR2*, *SIR3*, *HST1*, and *SUM1* open reading frames (ORFs) were deleted and replaced with *kanMX4* using a one-step PCR-mediated gene replacement protocol (36). *SIR4* and *HML* were deleted and replaced with *HIS3* and *LEU2*, respectively. The C-terminal ends of the *HST1*, *SUM1*, and *SIR3* open reading frames were tagged with 13 copies of the Myc epitope (EQKLISEEDL) at the endogenous chromosomal location by using PCR (34). Sir2 was previously tagged with 9 copies of the Myc tag (10). All gene deletions and Myc-tagged genes were confirmed by PCR.

Microarray gene expression analysis. Duplicate cultures (40 ml) of each strain were grown in YPD medium to an optical density at 600 nm (OD_{600}) of 0.35 to 0.55 (log phase). Total RNA was isolated using the hot acid phenol method (2) and resuspended in RNase-free water. Biotinylated cRNA for hybridizations was prepared from 4 μg total RNA according to the Affymetrix one-cycle eukaryotic target preparation protocol (GeneChip Expression Analysis Technical Manual 702232, rev. 3; Affymetrix). Following fragmentation, 4 μg of labeled cRNA was hybridized to Affymetrix Yeast Genome 2.0 GeneChip arrays using the manufacturer's recommended conditions. The GeneChip arrays were then scanned using an Affymetrix GeneChip scanner 3000. Raw data from the scanner (.cel format) was quantile normalized and the expression values estimated using GCRMA (18). We applied a modified *t* test using the limma package in Bioconductor to compare the results for mutant samples to those for the wild type (WT)

to identify differentially expressed genes (18). To arrive at lists of genes for every comparison, we first corrected for multiple hypothesis testing by applying a *f*alse *d*iscovery *r*ate (FDR) correction to the *P* values and used a 5% FDR cutoff.

In order to assess the significance of the enrichment in upregulated genes in the *npt1*Δ mutant and in the WT strain incubated with NAM (WT + NAM condition) in subtelomeric regions, we first applied a series of distance cutoffs from the chromosome ends, at 5, 10, 15, 20, and 25 kb. We compared the observed numbers of upregulated genes that were found within these distances to the chromosome ends in the *npt1*Δ mutant and in the WT + NAM condition to the numbers expected by chance. Specifically, we randomly sampled (100,000 times) for the number of genes that were significantly upregulated (134 for the *npt1*Δ mutant and 346 for the WT + NAM condition) from the total number of genes that had chromosomal coordinate information and positive $\log_2$-fold changes (2,037 for the *npt1*Δ mutant and 2,404 for the WT + NAM condition). We then calculated the number of genes that were found within the same 5 distance cutoffs shown above for each random sample, along with several statistical measurements, such as the mean of the random values, fold change of the observed value versus the mean of the random values, and *P* values.

Quantitative reverse transcriptase (RT) PCR assays. Total RNA was isolated from log-phase cultures for each strain tested. We used 1 μg of RNA for cDNA synthesis, performed by the addition of 1 μl of 10 mM deoxynucleoside triphosphates (dNTPs) and 1 μl oligo$(dT)_{12–18}$ (0.5 μg/μl) and incubation at 65°C for 5 min, followed by a quick chill on ice. A master mix of 4 μl of 5× First-Strand buffer (Invitrogen), 2 μl of 0.1 M dithiothreitol (DTT) was added to the sample, and then the mixture was incubated at 42°C for 2 min. SuperScript II reverse transcriptase (200 units; Invitrogen) was added to the reaction mixture (final reaction mixture volume of 10 μl) and incubated for 50 min at 42°C, followed by a 15-min incubation at 70°C to inactivate the enzyme. One microliter of RNaseH (2 units; Invitrogen) was added to the reaction mixture, and the mixture was further incubated at 37°C for 20 min. A 100-fold dilution of the resulting cDNA was analyzed by real-time PCR of a 20-μl reaction mixture volume in an Applied Biosystems 7300 real-time PCR system using SYBR green PCR Mastermix (Applied Biosystems). The oligonucleotide primer sequences are provided in Table S2 in the supplemental material. The test mRNA transcript levels were normalized to *ACT1* transcript levels. To determine the fold induction, gene transcript levels in the mutant strains were normalized to the levels in the wild-type strain. Results reflect the average fold induction (relative to the induction in the wild-type strain). Where indicated in the figures, the standard deviation was calculated from the differences from the mean of the fold induction in three independent cultures.

Chromatin immunoprecipitation (ChIP) assays. Log-phase yeast cultures (200 ml) in YPD were cross-linked with 0.5% formaldehyde for 20 min at 30°C. Cells were pelleted by centrifugation and washed 2 times with cold Tris-buffered saline. The cells, in 0.6 ml of FA-140 lysis buffer (50 mM HEPES, 140 mM NaCl, 1% Triton X-100, 1 mM EDTA, 0.1% sodium dodecyl sulfate [SDS], 0.1 mM phenylmethylsulfonyl fluoride [PMSF], 2 mM benzamidine, 1× protease inhibitor cocktail; Sigma), were lysed with glass beads and a Mini-BeadBeater (Biospec Products). The cell lysate was drawn off the beads, sonicated seven times for 45 s each at a setting of 30% output and 90% duty cycles for 10 pulses, and spun for 10 min in a microcentrifuge. Equivalent amounts of lysate (2.5 mg protein) were incubated overnight at 4°C with 2 μg of anti-Myc antibody (9E10). Samples were incubated with 60 μl of protein G-agarose-salmon sperm DNA for 1 h at 4°C and then washed (wash 1, twice with 1 ml of FA-140; wash 2, twice with 1 ml of FA-500 [the buffer was the same as FA-140 except that the NaCl concentration was increased to 500 mM]; and wash 3, twice with 1 ml LiCl solution containing 10 mM Tris-HCl, pH 8.0, 250 mM LiCl, 0.5% NP-40, 0.5% sodium dodecyl sulfate, 1 mM EDTA). DNA was then eluted from the beads 2 times with 75 μl of elution buffer (5× TE plus 1% SDS). The combined DNA solution was incubated at 65°C overnight to reverse the cross-linking. The purified DNA samples were analyzed by quantitative real-time PCR, and the results compared to a standard curve prepared from the input DNA. The amounts of immunoprecipitated DNA from the experimental promoters (*THI4* and *THI71*) and a control promoter (*ATS1*) were determined relative to the input DNA. The oligonucleotide sequences used are provided in Table S2 in the supplemental material. Standard deviations were calculated from the results for three independent biological replicates.

Calculation of intracellular NAD^+ levels. The determination of relative NAD^+ levels in various strains and conditions was performed using a fluorescent NAD/NADH detection kit (Cell Technology, Inc.). Yeast cells were inoculated into 40 ml YPD medium and grown to log phase (OD_{600} of ~0.5). A quantity of 2×10^6 cells was collected from each culture and washed twice with 2 ml of phosphate-buffered saline (PBS). After removal of the final supernatant, the cell pellet was resuspended into 200 μl of the NAD extraction buffer supplied in the kit. Next, 200 μl of the NAD/NADH lysis buffer was added, followed by glass beads (~0.5 ml). The cells were lysed in a Mini-BeadBeater (7 times for 45 s with 1-min intervals on ice). The cell lysates were collected, transferred to 1.5-ml microcentrifuge tubes, and then incubated at 60°C for 15 min. After being heated, the samples were immediately cooled on ice. One hundred microliters of the kit-supplied reaction buffer and 200 μl of NADH extraction buffer were added to neutralize the samples. The tubes were vortexed and centrifuged at 5,000 × *g* for 5 min to clarify the supernatants. Fifty microliters of each sample was added to individual wells of a black 96-well plate. Next, we added 100 μl of a reaction cocktail consisting of 98 μl NAD/NADH reaction buffer, 1 μl of the reconstituted enzyme mix, and 1 μl of NADH detection reagent to all the wells. Each sample was run in triplicate. After incubation at room temperature in the dark for 1.5 h, a reading was taken with a plate reader set for excitation at 530 to 570 nm and emission at 590 to 600 nm.

Thiamine measurements. Yeast cultures (200 ml YPD) were grown to log phase (OD_{600} of ~0.5). Cultures were transferred to ice, and cells collected by centrifugation in a Sorvall SLA-1500 rotor at 6,000 rpm for 5 min at 4°C. The cell pellets were washed with 30 ml of ice-cold water followed by 30 ml of ice-cold PBS and then resuspended in 2 ml PBS, and the volume was divided into 2 microcentrifuge tubes, followed by centrifugation at 14,000 × *g* for 15 s. The supernatants were discarded, and the cell pellets frozen in liquid nitrogen. The cell pellets were thawed on ice, resuspended in 0.6 ml PBS, and disrupted by adding 0.5 ml of glass beads and shaking 7 times for 45 s in a Mini-BeadBeater (Biospec Products) at 4°C, with 1-min intervals on ice. The lysates were harvested, and the cell debris removed by centrifugation.

Thiamine concentrations were determined by using a rapid high-performance liquid chromatography (HPLC) procedure (37). A stock solution of thiamine (approximate concentration, 1 mM) was prepared in 0.1 M hydrochloric acid as a calibrator. The exact concentration was determined by spectrophotometry at 246 nm, using a molar absorptivity of 14,200 liter mol^{-1} cm^{-1}. To measure thiamine, 20 μl of whole-cell extract was diluted in HPLC-grade water to a final volume of 1 ml. Aliquots (100 μl) of diluted yeast whole-cell-extract samples, water (blank), or thiamine standards of various concentrations were treated with 300 μl of methanol, immediately vortexed for 15 s, and then incubated at room temperature, protected from light, for 5 min. The samples were centrifuged at 2,000 × *g* for 5 min at 15°C, and the resulting supernatants (50 μl) were transferred to a 96-well microtiter plate preloaded with 50 μl of water per well. Immediately prior to injection into the HPLC, the samples were derivatized to thiochrome products by the addition of 50 μl of freshly prepared potassium ferricyanide in 15% (wt/vol) sodium hydroxide. The final concentrations were 0.2 mmol/liter for potassium ferricyanide and 5% (wt/vol) for sodium hydroxide. The microtiter plate was covered with sealing tape and placed into the precooled autosampler. Reverse-phase HPLC was performed as previously described on an Agilent 1200 series rapid-resolution LC system with the autosampler set at 10°C (37). An excitation wavelength of 375 nm was used, and thiamine detected at an emission wavelength of 435 nm. The thiamine concentrations in the diluted samples were determined by evaluating peak areas in comparison to the corresponding calibration curve. The actual whole-cell-extract sample concentrations were determined by adjusting for the appropriate dilution factor.

Microarray data accession number. The datasets from this study have been deposited in NCBI's Gene Expression Omnibus (14) and are accessible through GEO Series accession number GSE18488 (http://www.ncbi.nlm.nih.gov/geo/query/acc.cgi?acc=GSE18488).

RESULTS

Identifying genes that are differentially expressed when NAD^+ metabolic pathways are disrupted. We were initially interested in determining the degree of overlap in altered gene expression that occurs when sirtuins are inhibited by either a reduction in NAD^+ concentration or an accumulation of NAM. To reduce the NAD^+ concentration, we deleted *NPT1*, and to elevate the intracellular NAM concentration, we either deleted *PNC1* or added 5 mM NAM to the growth medium of the WT strain (WT + NAM condition). All three of these conditions were previously demonstrated to inhibit Sir2 *in vivo*, resulting in general heterochromatic silencing defects (7, 17, 51). As controls, we tested the effects of deleting *BNA1* or *TNA1*, which does not reduce the NAD^+ concentration or

TABLE 1. Enrichment in upregulated genes near telomeres

Genotype or growth condition	Distance from chromosome end (bp)	Total no. of upregulated genes[a]	No. of genes detected within window	Expected no. of genes (random)[b]	Fold enrichment over random no.	*P* value
WT + NAM	5,000	346	5	1.30	3.85	0.004
WT + NAM	10,000	346	18	3.59	5.01	<1e-05
WT + NAM	15,000	346	24	6.02	3.99	<1e-05
WT + NAM	20,000	346	31	8.17	3.80	<1e-05
WT + NAM	25,000	346	35	11.87	2.95	<1e-05
*npt1*Δ	5,000	134	2	0.53	3.77	0.094
*npt1*Δ	10,000	134	6	1.71	3.51	0.006
*npt1*Δ	15,000	134	11	2.76	3.98	1e-04
*npt1*Δ	20,000	134	16	3.67	4.36	<1e-05
*npt1*Δ	25,000	134	18	5.25	3.43	<1e-05
*pnc1*Δ	5,000	37	0	0.95	0	1
*pnc1*Δ	10,000	37	0	0.31	0	1
*pnc1*Δ	15,000	37	0	0.53	0	1
*pnc1*Δ	20,000	37	1	0.71	1.42	0.514
*pnc1*Δ	25,000	37	2	0.95	2.11	0.244

[a] Genes shown to be significantly upregulated. Analysis was restricted to genes with chromosomal coordinate information from the Bioconductor microarray analysis.
[b] Calculated from 100,000 iterations.

inhibit silencing when cells are grown in rich medium (51). Deleting *BNA1* blocks the *de novo* NAD^+ biosynthesis pathway (26), and deleting *TNA1* reduces nicotinic acid import from the growth medium (33). To assess the global transcriptional responses under each of these conditions, we grew the WT, *npt1*Δ, *pnc1*Δ, *bna1*Δ, and *tna1*Δ strains in YPD medium. The WT strain (ML1) was also grown in YPD supplemented with 5 mM NAM. Exponentially growing cells were harvested from each culture, and total RNA isolated. Northern blotting confirmed that the expression levels of *TNA1* and *BNA1* were both elevated in the *npt1*Δ strain, as predicted from the results of an earlier study (3), indicating that the strains in this background responded appropriately to the reduction in NAD^+ (data not shown).

Total RNA from 2 independent biological replicates of each strain or condition was next hybridized to Affymetrix gene arrays (Yeast Genome 2.0) that cover all annotated open reading frames. The microarray data were analyzed using a modified triple array error model (see Materials and Methods) to calculate the significance of the observed changes in mRNA levels. Gene expression levels with *P* values of less than 0.05 compared to the level in the WT (ML1) were considered differentially expressed. Overall, we identified 116 genes that were differentially expressed in the *pnc1*Δ mutant, 208 in the *npt1*Δ mutant, and 726 in the WT strain incubated with NAM (WT + NAM) (Fig. 1B). Only 1 gene (*SVS1*) was differentially expressed in the *bna1*Δ mutant, and no gene expression levels from the *tna1*Δ mutant were significantly changed (data not shown). Therefore, in rich-medium conditions, the contributions of the *de novo* NAD^+ biosynthesis pathway and the high-affinity nicotinic acid transporter to gene regulation are negligible. There was substantial overlap in differentially regulated genes between the three strongly affected conditions (Fig. 1B, left), with the largest intersection between the *npt1*Δ mutant and the WT + NAM condition (77% of the *npt1*Δ-affected genes). If only upregulated genes were taken into account, then 86% of the *npt1*Δ-affected genes overlapped with genes affected by the WT + NAM condition (Fig. 1B, right). Surprisingly, less than 40% of the *pnc1*Δ-affected genes overlapped with genes affected by the WT + NAM condition, suggesting that Pnc1 may have additional roles in gene expression independent of its effects on NAM clearance. Another possible reason for this small amount of overlap is that adding 5 mM NAM to the growth medium raises the intracellular NAD^+ concentration (39), which could affect an additional subset of genes.

Regulation of thiamine biosynthesis genes by the intracellular NAD^+ and NAM concentrations. Defects in the NAD^+ salvage pathway have previously been shown to impair silencing of telomeric reporter genes (54). It was therefore possible that many genes upregulated in the microarray data sets would be located near telomeres. Indeed, there was a significant enrichment in upregulated genes in the *npt1*Δ mutant and the WT + NAM condition in subtelomeric regions compared to what would be expected by chance (Table 1), consistent with a telomeric silencing defect. However, despite the enrichment, most of the differentially regulated genes (including those upregulated) were not located within 25 kb of a telomere, suggesting that silencing-independent transcriptional effects were also at play. Comprehensive lists of genes that were significantly up- or downregulated in each condition are provided in Tables S3, S4, and S5 in the supplemental material. The datasets have also been deposited in NCBI's Gene Expression Omnibus (14) and are accessible through GEO Series accession number GSE18488 (http://www.ncbi.nlm.nih.gov/geo/query/acc.cgi?acc=GSE18488).

Further analysis of the microarray datasets revealed a significant amount of overlap between the genes upregulated by the addition of NAM or by the *npt1*Δ mutation and genes previously shown to be upregulated by deletions of small repressive domains within the histone H3 or H4 N-terminal tails (45, 46). For example, 133 out of 433 genes upregulated by the addition of NAM (30.7%) were also upregulated in one or both of the histone tail mutants (Fig. 1C). For the *npt1*Δ-upregulated genes, 73 out of 175 (41.7%) overlapped with the histone mutant gene sets (Fig. 1C). These results suggested that a substantial amount of the gene repression mediated by the H3 and H4 repressive domains is dependent on sufficient

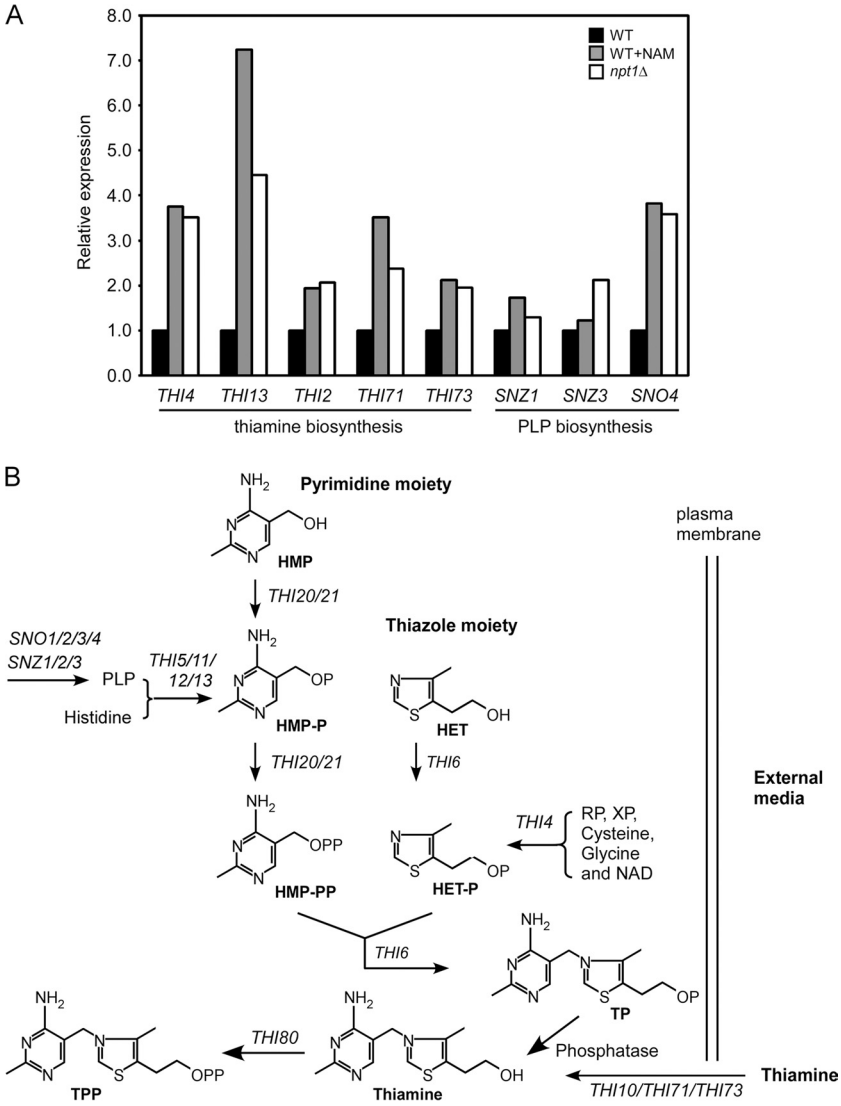

FIG. 2. Thiamine and pyridoxal 5′-phosphate (PLP) biosynthesis genes are upregulated by conditions that inhibit sirtuins. (A) Validation by quantitative RT-PCR analysis of mRNA expression from several thiamine and pyridoxal biosynthesis genes identified from the microarray analysis relative to *ACT1* expression. The test gene/*ACT1* ratio was normalized to 1.0 for each gene in the WT strain. Values are the averages of the results for the two independent RNA samples used for the microarray analysis. (B) Schematic diagram of thiamine biosynthesis and transport in *Saccharomyces cerevisiae*. Abbreviations: HMP, 4-amino-5-hydroxymethyl-2-methylpyrimidine; HMP-P, 4-amino-5-hydroxymethyl-2-methylpyrimidine monophosphate; HMP-PP, y-amino-5-hydroxymethyl-2-methylpyrimidine diphosphate; HET, 5-(2-hydroxyethyl)-4-methylthiazole; HET-P, 5-(2-hydroxyethyl)-4-methylthiazole phosphate; PLP, pyridoxal 5′-phosphate; RP, D-ribulose 5-phosphate; TP, thiamine phosphate; TPP, thiamine pyrophosphate; XP, D-xylulose 5-phosphate.

intracellular NAD^+ and, most likely, one or more of the sirtuins. Among the overlapping genes were those that function in *de novo* NAD^+ biosynthesis (the *BNA* genes), as well as several involved in thiamine (vitamin B1) and pyridoxal 5′-phosphate (PLP; vitamin B6) biosynthesis. As mentioned above, the elevated expression of *BNA1* and *TNA1* was confirmed by Northern blotting (data not shown). To validate the microarray results for thiamine and PLP biosynthesis genes, we selected several that were shown to be upregulated in both the *npt1*Δ mutant and the WT + NAM condition for analysis using quantitative real-time RT-PCR on the duplicate total RNA samples used for the microarray hybridizations. As shown in Fig. 2A, the average expression level for each *THI* gene tested was elevated compared to the WT expression level (normalized to 1.0). For the PLP biosynthesis genes tested, *SNO4* was clearly upregulated by both conditions, but the effects on *SNZ1* and *SNZ3* were modest and variable. This led us to further characterize the regulation of several thiamine biosynthesis genes.

NAD^+ and PLP are both utilized as substrates for thiamine biosynthesis in yeast (Fig. 2B), and based on our microarray expression profiling data, the expression of genes in each of these biosynthetic pathways appears to be regulated by conditions that inhibit sirtuins. Hst1 had previously been shown to repress the *de novo* NAD^+ biosynthesis genes (3), which made it a primary candidate for regulating genes in the thiamine and PLP biosynthesis pathways. However, the thiamine genes were

not identified as being upregulated in an *hst1*Δ mutant in that study. One of the key differences besides strain background between the earlier study and ours was the type of medium. We used rich YPD medium, and the earlier study used synthetic complete (SC) medium (3). Compared to YPD medium, SC medium contains relatively low concentrations of thiamine and the NAD^+ precursor nicotinic acid, thus making it possible that thiamine gene expression was already derepressed in SC due to induction of the thiamine biosynthesis pathway. As shown in Fig. 3A, the expression levels of *THI13*, *THI4*, *THI2*, and *THI73* were between 6- and 100-fold higher in SC medium than in YPD medium. Furthermore, adding 5 mM NAM or deleting *NPT1* had no effect on the expression of *THI4* or *THI13* in SC medium (Fig. 3B), while it raised their expression levels 3- to 4-fold in YPD medium (Fig. 3C). The *THI* genes are therefore strongly repressed in rich YPD medium, making them responsive to either a decrease in NAD^+ concentration or an increase in NAM concentration.

To confirm that a decrease in NAD^+ caused by the *npt1*Δ mutant was at least partially responsible for the elevated *THI* gene expression, we first supplemented the YPD medium with 10 μM nicotinamide riboside and examined *THI4* expression as an example. This concentration of nicotinamide riboside was previously shown to elevate the NAD^+ concentration in an exponentially growing *npt1*Δ mutant (4), which we also observed in this current study (Fig. 3D). As predicted, nicotinamide riboside did restore the repression of *THI4* in the *npt1*Δ mutant but had no effect on *THI4* expression in the WT strain, probably because the already high NAD^+ concentration in the WT strain was unaffected by the addition of the compound (Fig. 3E). Despite the known reduction in NAD^+ concentration observed in SC medium-grown cells compared to the concentration in YPD medium-grown cells (51), this was unlikely to account for most of the difference in *THI* gene expression in the two types of medium. Indeed, titration of the thiamine concentrations in SC medium resulted in a remarkable 5,000-fold range in the *THI4* expression level (Fig. 3F). When thiamine was maintained in the linear range for *THI* gene expression (100 nM), removing nicotinic acid to lower the NAD^+ concentration even further than normal did result in a statistically significant elevation in *THI4* expression (Fig. 3G). From these results, it appears that a high NAD^+ concentration is important for maintaining *THI* genes in a fully repressed (basal) state when nutrients are abundant but thiamine concentration is the key player in the activation of these genes when nutrients are scarce.

Thiamine gene expression is directly repressed by Hst1 and Sir2. To determine whether the NAD^+-dependent sirtuins are involved in repressing the *THI* genes, we first quantified the effects of deleting *SIR2* and the *HST* genes on *THI* gene expression in cells growing in YPD. Deleting *SIR2* resulted in small but reproducible increases in expression for each of the *THI* genes tested (Fig. 4A to D). Similar increases were observed when *SIR3* or *SIR4* was deleted, suggesting that the SIR silencing complex plays a minor role in *THI* gene repression. The exception was *THI13*, which showed a larger, 2.5- to 3-fold increase in expression when any subunit of the SIR complex was disrupted (Fig. 4B). Cells lacking the SIR complex are defective for silencing at telomeres and the *HML*/*HMR* loci (35), which could explain why the subtelomeric *THI13* gene was upregulated. By derepressing the *HML* and *HMR* loci, haploid *sir* mutant cells such as these are made to undergo transcriptional reprogramming that mimics diploid strains, which can have indirect effects on specific phenotypes, such as nonhomologous end-joining of DNA breaks (30). It was therefore possible that the increased *THI* gene expression could be an indirect effect. To test this possibility, *HML* was deleted from the *MAT***a** WT and *MAT***a** *sir2*Δ strains. The lack of *HML* eliminates the possibility that inappropriate expression of both *HMR* and *HML* contributes to the *sir2*Δ phenotype. As shown in Fig. 4E and F, the lack of *HML* did not block the elevated expression of *THI4* and *THI13* when *SIR2* was deleted, ruling out an indirect effect at this level.

Among the *HSTs*, only the deletion of *HST1* caused derepression of the *THI* genes (data not shown). This derepression was also stronger than the effect of deleting *SIR2*, at least for the *THI4*, *THI71*, and *THI73* genes (Fig. 4A, C, and D). For the subtelomeric *THI13* gene, the effects on its derepression of deleting *SIR2* and *HST1* were similar (Fig. 4B). Hst1 is recruited to targeted gene promoters in a complex with Rfm1 and Sum1 (40, 49, 60). For *THI4*, *THI13*, and *THI73*, the *sum1*Δ mutation caused gene derepression that was similar to the effect of the *hst1*Δ mutation (Fig. 4A, B, and D). An exception was *THI71* (Fig. 4C), where the *sum1*Δ mutant showed significantly greater expression than the *hst1*Δ mutant. It is possible that Sum1 recruits another unidentified corepressor to the *THI71* promoter or has repressive activity on its own at this gene. For *THI4*, *THI13*, and *THI73*, the *sir2*Δ *hst1*Δ double mutant combination was additive, suggesting that the SIR complex and Hst1/Sum1 complex associate independently with certain *THI* gene promoters.

Chromatin immunoprecipitation (ChIP) was used to test whether Myc-tagged Sir2 and Hst1 associate with any of the *THI* genes. *THI4* and *THI71* were chosen as representatives because they are not located near a telomere. In addition, *THI4* repression was similarly affected by the *hst1*Δ and *sum1*Δ mutations (Fig. 4A), while *THI71* expression differed in the two mutants (Fig. 4C). Three different primer sets (A, B, and C) were initially chosen for each gene. Set A was farthest upstream from the start codon (~800 bp). Set B was located at an intermediate distance (~400 to 500 bp), and set C was within the coding region (Fig. 5A). An earlier study found that Sir2 and Hst1 did not associate with the *ATS1* gene (21), so its promoter sequence was used as a negative control. As shown in Fig. 5B, Myc-tagged Sir2 was enriched at *THI4* compared to the *ATS1* signal, although, surprisingly, the enrichment was greatest at the most distant segment (set A). Myc-tagged Sir3 also associated with this upstream region of the *THI4* promoter with a ChIP signal comparable to that of Sir2-Myc (Fig. 5C), suggesting that the SIR complex can be recruited to specific genes other than the known heterochromatic loci in yeast. Myc-tagged Hst1 showed stronger enrichment than Sir2 on the *THI4* gene, with the strongest signal located at position A (Fig. 5B). The greater enrichment for Hst1 was consistent with its larger effect on *THI4* repression. Surprisingly, Sum1 was only modestly enriched on the *THI4* promoter in comparison to the *ATS1* signal. With an untagged strain, there were no differences in ChIP signal between the *THI* gene promoter regions and the *ATS1* control (data not shown).

The association pattern on the *THI71* gene was different

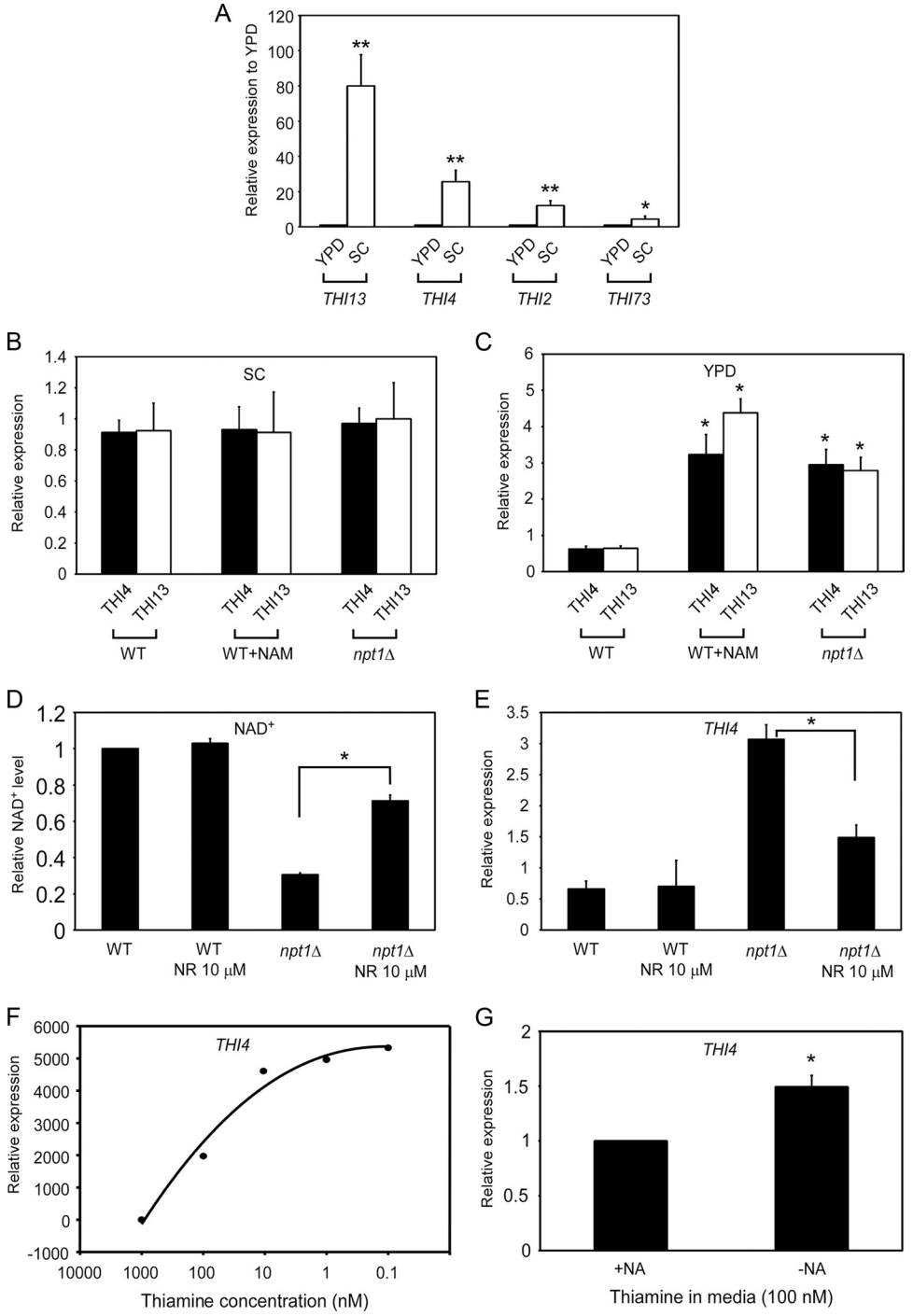

FIG. 3. Effects of growth media and NAD^+ concentrations on *THI* gene expression. (A) Quantitative RT-PCR analysis of *THI13*, *THI4*, *THI2*, and *THI73* mRNA levels in SC medium compared to their levels in YPD medium. Expression levels in YPD were normalized to 1.0. (B) *THI4* and *THI13* expression in the WT strain without or with the addition of 5 mM NAM and in the *npt1*Δ mutant. Cells were grown in SC medium. (C) *THI4* and *THI13* expression in the WT strain without or with the addition of 5 mM NAM and in the *npt1*Δ mutant. Cells were grown in YPD medium. (D) Effects of 10 μM nicotinamide riboside (NR) on the relative intracellular NAD^+ levels in the WT and *npt1*Δ strains growing in YPD medium. Results for the WT without NR addition were set to 1. (E) Effects of 10 μM NR on *THI4* expression in the WT and *npt1*Δ mutant strains growing in YPD medium. (F) *THI4* expression levels in SC medium containing the indicated concentrations of thiamine. (G) Increased *THI4* expression caused by a lack of nicotinic acid (NA) in SC medium containing 100 nM thiamine (the linear range for *THI4* expression). In each panel, changes with a *P* value of <0.05 are indicated by one asterisk, and *P* values of <0.005 are indicated by two asterisks. Error bars show standard deviations.

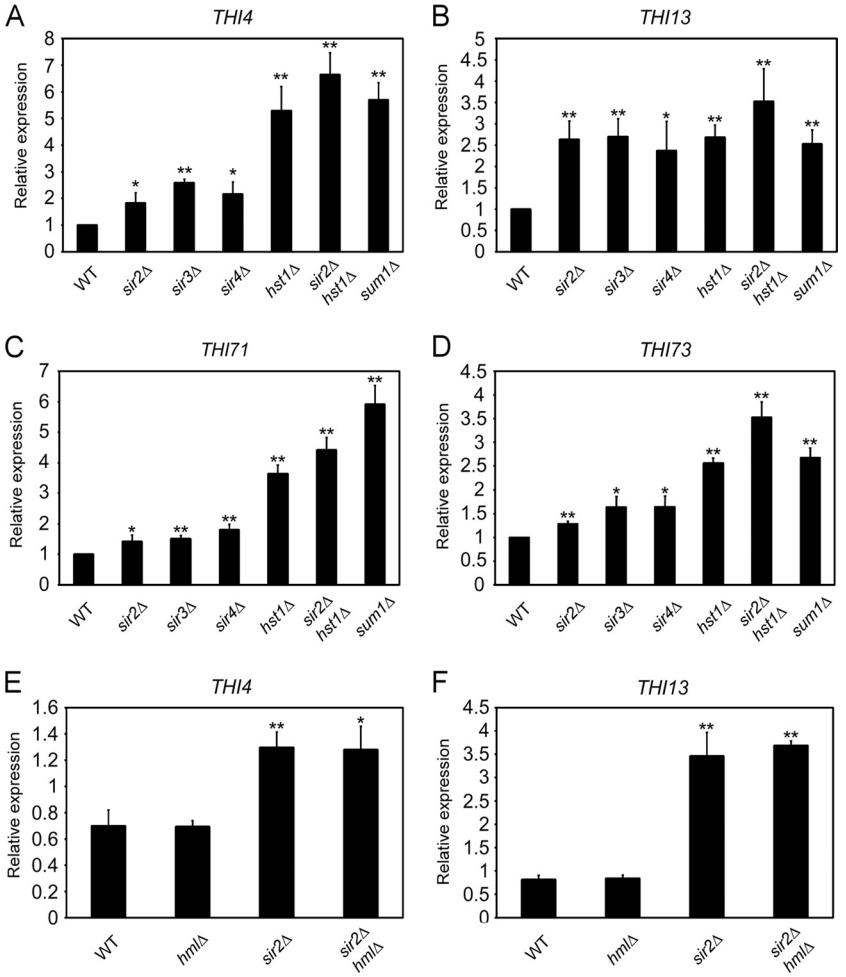

FIG. 4. Repression of *THI* genes by the SIR and Hst1/Sum1 histone deacetylase complexes. (A to D) Results of quantitative RT-PCR analysis of *THI4*, *THI13*, *THI71*, and *THI73* mRNA levels. Expression is relative to the *ACT1* RNA level. Results for the WT were normalized to 1.0 for each gene. (E and F) Results of quantitative RT-PCR measurement of *THI4* and *THI13* mRNA levels in WT and *sir2*Δ strains with the *HML* locus either intact or deleted. *P* values of <0.05 are indicated by an asterisk. *P* values of <0.005 are indicated by a double asterisk. Error bars show standard deviations.

than that of *THI4*. Hst1 and Sum1 were both strongly associated with *THI71*, with the enrichment for Sum1 binding being even greater than that for Hst1 (Fig. 5D), thus correlating with the more robust derepression effect on this gene of deleting *SUM1*. Interestingly, the area of greatest enrichment was again at the promoter-distal region (set A). Relatively little Sir2 associated with the *THI71* promoter (Fig. 5D), consistent with the very weak effect on *THI71* repression of deleting *SIR2* (Fig. 4C). Despite the difference in *THI71* expression caused by the *hst1*Δ and *sum1*Δ mutations, Sum1 was still required for Hst1 to associate with the *THI71* promoter at position A (Fig. 5E). The unexpected enrichment for Hst1, Sir2, and Sum1 at a position ~800 bp upstream of the transcriptional start site led us to examine binding even further upstream (position D). For the *THI4* gene, Myc-tagged Sir2, Hst1, and Sum1 did not bind significantly at this position compared to their binding in the *ATS1* control (Fig. 5F). For *THI71*, there was some binding at position D, but it was not as strong as the peak at position A (Fig. 5G). We also tested *THI4* for binding at the traditional transcriptional promoter region for yeast genes, ~150 to 200 bp upstream of the start site (position E), but there was no significant enrichment for the tagged proteins (Fig. 5F). We were unable to detect any difference in Sir2 or Hst1 binding to position A when cells were grown in the presence or absence of thiamine (data not shown). Sir2 was previously shown to substitute for Hst1 in complex with Sum1 when Hst1 was deleted (21). However, our data suggest that, for some of the thiamine genes, both the SIR complex and the Hst1/Sum1/Rfm1 complex can independently associate with a region ~800 bp upstream of the transcription start site to fully repress basal transcription when NAD^+ levels are sufficiently high.

We were next interested in whether there were differential effects on histone acetylation when Sir2 or Hst1 was absent, using anti-H3-K9/K14-acetyl and anti-H4 pan-acetyl antibodies in quantitative ChIP assays. *THI4* and *THI71* primers (peak position A) were chosen to match with the ChIP data collected for Sir2 and Hst1 binding. H4 acetylation at *THI4* was elevated in the *sir2*Δ, *hst1*Δ, and *sir2*Δ *hst1*Δ mutants, but H3 acetylation was unaffected (Fig. 6A). This was in sharp contrast with the *THI71* promoter result, where the *hst1*Δ mutation caused hyperacetylation on both H3 and H4 (Fig. 6B). We were unable to detect any significant change in H3 or H4 acetylation for

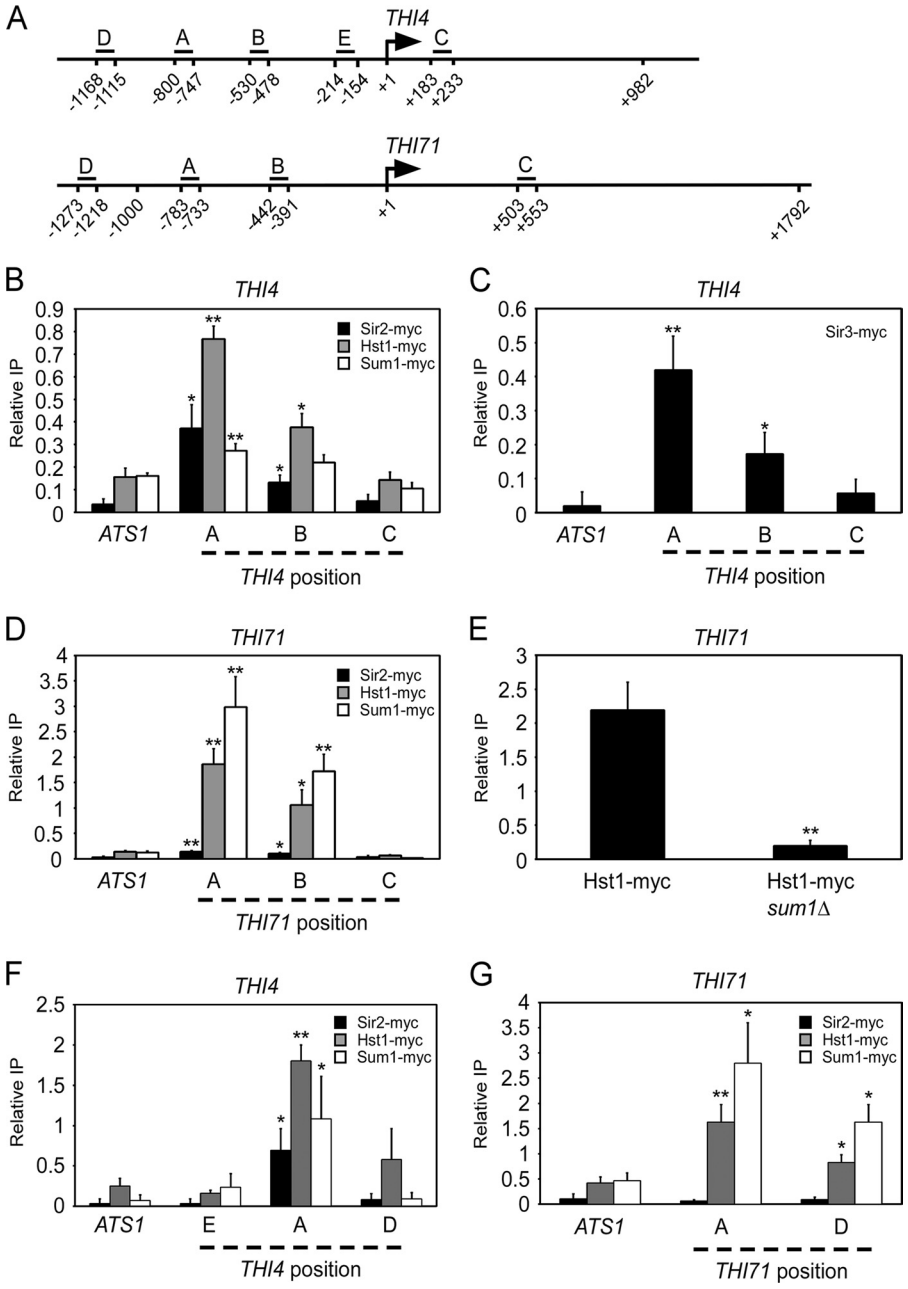

FIG. 5. Chromatin IP analysis of Sir2, Hst1, Sum1, and Sir3 association with the *THI4* and *THI71* genes. (A) Schematic diagram indicating the positions of PCR primers used to detect immunoprecipitated DNA. Base pair positions relative to the transcriptional start site are provided. (B) Association of Myc-tagged Sir2, Hst1, and Sum1 with a region upstream of the traditional *THI4* promoter region (position A). The *ATS1* promoter is used as a negative control that does not associate with Sir2, Hst1, or Sum1. "Relative IP," on the *y* axis, indicates the ratio between the immunoprecipitated DNA's PCR signal and the input DNA's PCR signal. (C) Chromatin IP results showing association of Myc-tagged Sir3 with the same upstream *THI4* region (position A). (D) Chromatin IP results showing Myc-tagged Sir2, Hst1, and Sum1 association with the *THI71* gene. (E) Chromatin IP results showing that Hst1 association ~750 bp upstream of the *THI71* transcription start site (position A) requires *SUM1*. (F) Chromatin IP results showing that Myc-tagged Sir2, Hst1, and Sum1 binding to *THI4* does not extend close to the transcription start site (position E) or ~1,150 bp upstream (position D). (G) Binding does extend further upstream from the *THI71* start site (position D). In each panel, changes with a *P* value of <0.05 are indicated by one asterisk, and *P* values of <0.005 are indicated by two asterisks. Error bars show standard deviations.

THI71 in the *sir2*Δ mutant (Fig. 6B). Therefore, even when Hst1 is present, Sir2 is an active histone H4 deacetylase at the *THI4* promoter but not at *THI71*. Additionally, the specificity of Hst1 as an H3 and/or H4 deacetylase varies depending on the *THI* gene targeted.

Intracellular thiamine concentration is controlled by Npt1 and Hst1. Since the thiamine biosynthesis genes are generally repressed when cells are grown in rich YPD medium, we considered the possibility that derepression of the *de novo* thiamine biosynthesis and transport genes caused by deletion of

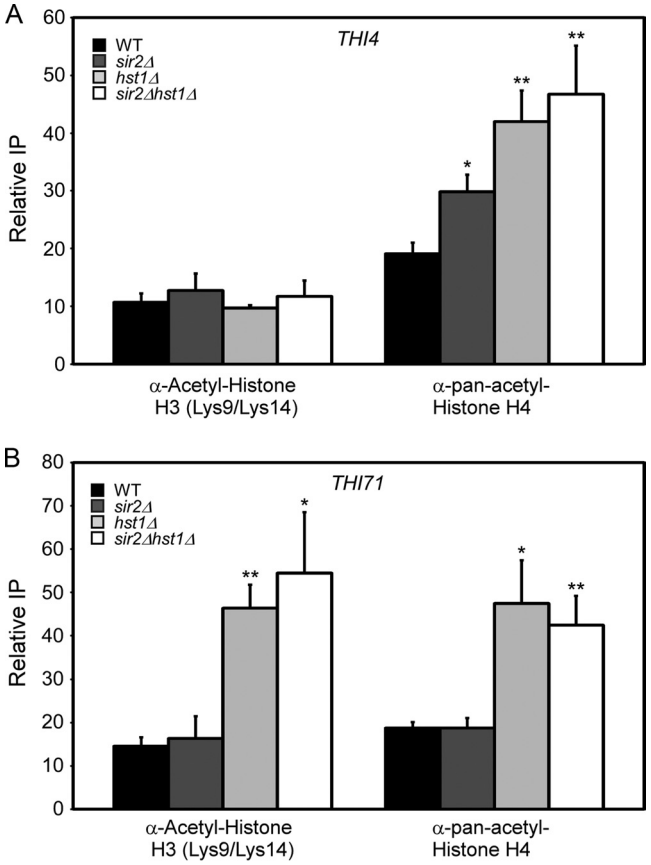

FIG. 6. Effects of *SIR2* and *HST1* on histone H3 and H4 acetylation at the *THI4* and *THI71* promoters. (A) Chromatin IP analysis of H3 and H4 acetylation at the *THI4* promoter in WT, *sir2*Δ, *hst1*Δ, and *sir2*Δ *hst1*Δ strains. (B) Chromatin IP analysis of H3 and H4 acetylation at the *THI71* promoter. In each panel, changes with a *P* value of <0.05 relative to results for the WT are indicated by one asterisk, and *P* values of <0.005 are indicated by two asterisks. Error bars show standard deviations. α, anti.

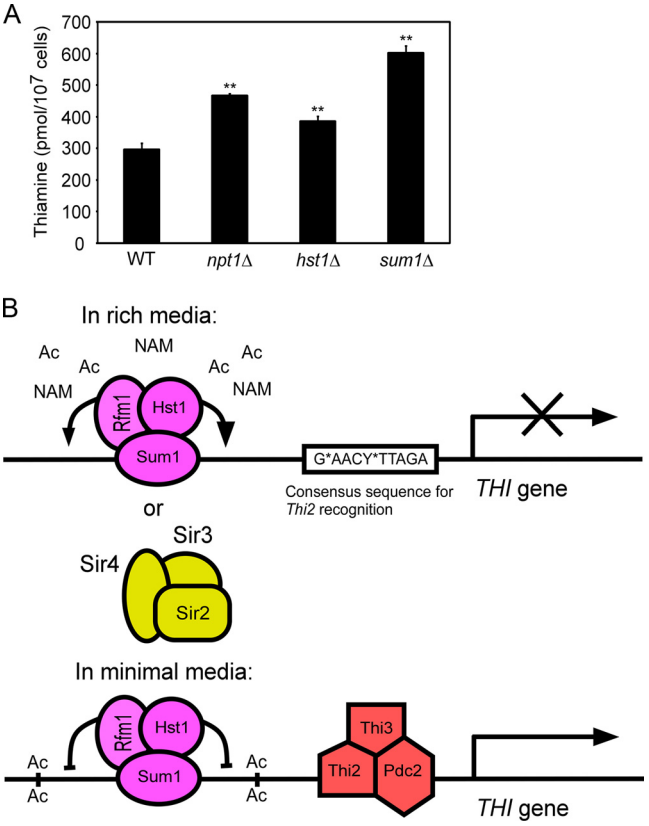

FIG. 7. NAD^+-mediated regulation of thiamine biosynthesis. (A) Intracellular thiamine levels in WT, *npt1*Δ, *hst1*Δ, and *sum1*Δ strains as measured by HPLC. (B) Model of *THI* gene regulation by the Hst1/Rfm1/Sum1 complex and the SIR complex (Sir2, Sir3, and Sir4). High intracellular NAD^+ concentrations in cells grown in nutrient-rich YPD medium promote local histone deacetylation by one or both complexes when they are bound to a site upstream of the consensus Thi2 recognition site in the promoter region. High thiamine in the YPD also prevents binding of the Thi2/Thi3 transcriptional activator complex, which, along with Pdc2, activates the *THI* genes when thiamine concentrations are low. The result is tight repression of basal *THI* gene expression. The histone deacetylation also generates nicotinamide (NAM) as a by-product of the sirtuin-mediated reaction. In minimal medium, low thiamine levels facilitate binding of Thi2/Thi3/Pdc2 to the *THI* gene promoter to activate transcription. In parallel, decreased intracellular NAD^+ levels reduce Hst1 deacetylation activity by the bound Hst1/Rfm1/Sum1 or SIR complex, also promoting increased *THI* gene expression. Error bars show standard deviations.

NPT1 or *HST1* would result in elevated intracellular thiamine concentrations. To test this hypothesis, HPLC analysis of whole-cell extracts was used to measure intracellular thiamine concentrations from the WT, *npt1*Δ, *hst1*Δ, and *sum1*Δ strains. As shown in Fig. 7A, the thiamine concentration was significantly elevated in each of these mutants, with the largest increase observed for the *sum1*Δ mutation, consistent with the relatively large increases in *THI* gene expression caused by the lack of Sum1. The modest increases in *THI* gene expression (of some genes) caused by the loss of *SIR2* were not sufficient to trigger a detectable change in thiamine concentration (data not shown). From these results, we conclude that in order to maintain proper cellular thiamine homeostasis in rich medium, a sufficient concentration of NAD^+ must be achieved to keep basal *THI* gene transcription repressed via the Hst1/Sum1 complex. Some *THI* genes, including those that are subtelomeric, also require the SIR complex for full repression.

DISCUSSION

Sirtuins as repressors of basal *THI* gene expression. There are three transcription factors in *S. cerevisiae* known to activate *THI* genes when thiamine levels are low, Thi2, Thi3, and Pdc2 (22, 41). Thi3 appears to act as the TPP sensor because it has a TPP binding pocket, which when mutated to block binding, converts Thi3 into a constitutive transcriptional activator (44). In addition, *thi80* mutations that reduce intracellular TPP levels constitutively activate the *THI* genes (42). Thi2 and Thi3 interact through a mechanism that is partly dependent on TPP, and deletion of these two genes results in similar global gene expression changes, suggesting that they work together (44). Pdc2 also activates the *THI* genes but may coordinate expression under metabolic conditions other than thiamine deprivation (41).

While the activation of *THI* genes in *S. cerevisiae* has been significantly characterized, the mechanisms of repression are

poorly understood. Our data implicate the NAD^+-dependent histone deacetylase Hst1 as a repressor of basal *THI* gene transcription. When thiamine levels are high, as is the case in YPD medium, full repression of the *THI* genes is dependent on having sufficiently high NAD^+ concentrations to support Hst1-mediated histone deacetylation as part of the Hst1/Sum1/Rfm1 complex. Some *THI* genes, including *THI4* and the subtelomeric *THI13* gene, are also maintained in the fully repressed state by Sir2 as part of the SIR silencing complex (see the model in Fig. 7B). To our knowledge, this is the first characterization of specific basal repressors for *S. cerevisiae* thiamine gene expression. Interestingly, the changes in transcriptional derepression observed in response to NAM or deletion of *NPT1* overlapped significantly with those observed when amino acids 30 to 37 of the histone H2B N terminus or 16 to 20 of the H2A N terminus were deleted (45, 46) (Fig. 1C). *THI4* and other *THI* genes were included in the overlap. Hst1 and Sir2 are therefore potential candidates for carrying out H2A and H2B lysine deacetylation that occurs on these histone tails (55). When thiamine is depleted from the environment, Thi2, Thi3, and Pdc2 likely recruit transcriptional coactivators with histone acetyltransferase activity to the consensus thiamine regulatory sequence ~150 bp upstream of the start site, overriding the repressive effects of the sirtuins, which bind further upstream (Fig. 7B). This is consistent with a role for Hst1 and Sir2 in repressing basal gene expression, not activated expression. In addition to the specific deacetylation carried out by Hst1 and sometimes Sir2, global histone deacetylation carried out by Hda1 may also contribute to the basal repression of some *THI* genes, as we have determined that deletion of *HDA1* induces a 2-fold increase in *THI4* expression (M. Li, unpublished data).

Sirtuin target genes. Hst1 and Sum1 are repressors of genes involved in *de novo* NAD^+ biosynthesis and nicotinic acid transport (3) and have been shown to be required for normal H3 and H4 deacetylation at the *BNA5* promoter (49), suggesting that a similar mechanism may be shared between these classes of genes and the *THI* genes. However, Sir2 was not implicated in repression of *de novo* NAD^+ biosynthesis genes in the earlier studies. Another distinction is that Hst1/Sum1 were found to associate within the proximal promoter region at *BNA2*, *BNA5*, and *TNA1* (3, 49), whereas we observed peak Hst1/Sum1 binding ~800 bp upstream from the transcription start site for both *THI4* and *THI71*. Sir2 also associated specifically at this position upstream of *THI4*. This difference in the position of Hst1/Sum1 binding likely reflects the presence of a consensus binding site for Thi2/Thi3/Pdc2 within the promoters of the *THI* genes that is missing from the NAD^+ biosynthesis genes. Despite the enrichment for Hst1/Sum1 at *THI4* and *THI71*, we were unable to detect a Sum1 consensus binding site at or near the position of binding using PatMatch on the *Saccharomyces* Genome Database website. For *THI4*, the −800 upstream site overlaps with a $tRNA^{Gly}$ gene (*SUF4*) and some Ty1 long terminal repeats, but since the *THI71* binding site does not contain these elements, it is unlikely that they are critical for the Sum1/Hst1 enrichment. We propose that Hst1/Sum1 or Sir2 binding upstream from the Thi2/Thi3/Pdc2 binding site facilitates full repression of the *THI* genes in rich medium while still allowing a rapid activation response due to reduced thiamine concentrations (Fig. 7B).

In addition to NAD^+ and thiamine biosynthesis genes, Hst1 is also targeted to the promoters of several middle sporulation genes (60). In this case, Sir2 can substitute for Hst1 in the Sum1 complex to repress transcription, but only when Hst1 is missing (21). Deleting *SIR2* had no effect on transcription of the middle sporulation genes unless *HST1* was also deleted (21). Sir2 and Hst1 are 63% identical; their genes are proposed to have derived from a whole-genome duplication event in a *Saccharomyces cerevisiae* ancestor approximately 100 million years ago (13, 24, 59) and likely retained some shared affinity for Sum1 (21). For certain *THI* genes, such as *THI4*, we have determined that both the SIR and the Hst1/Sum1 complex can independently associate with the promoters to repress transcription and that deleting *SIR2*, *SIR3*, or *SIR4* (the SIR complex) modestly increases the expression of the *THI* genes even when *HST1* is present. It remains unclear whether the SIR complex and the Sum1-Hst1 complex bind to the *THI4* promoter simultaneously, although since the peak association for each occurs at the same region upstream of the promoter, it is more likely that they do not bind at the same time (Fig. 7B). It is possible that having alternative repressive complexes is beneficial to potential epigenetic regulation within a cell population that is attempting to adapt to variations in thiamine and nicotinic acid concentrations.

Previous microarray analysis of chromatin immunoprecipitations (ChIP-chip) with anti-acetyl-histone antibodies found that the loss of Sir2 resulted in elevated acetylation at subtelomeric regions generally less than 4 kb from the telomeric ends (50). Genes within these regions are therefore likely regulated by the SIR complex-mediated telomeric silencing process. *THI13* and other genes in its family (*THI5*, *THI11*, and *THI12*) are considered to be subtelomeric, although they do not fall within 4 kb of the chromosome end. We found that *THI13* was equally derepressed by the deletion of either *SIR2* or *HST1*, suggesting that this class of *THI* genes is controlled by both the telomeric silencing mechanism via the SIR complex and specific promoter targeting via the Sum1/Hst1 complex. Another subtelomeric gene, *FLO10*, is similarly epigenetically repressed by Hst1 and the SIR complex, as well as by another sirtuin, Hst2 (20). *FLO10* is also repressed by the class II histone deacetylase Hda1 (20), which has been shown to repress multiple clusters of subtelomeric genes known as HAST (Hda1-affected subtelomeric) domains (50). *THI4* is not subtelomeric, yet it is still significantly repressed by Sir2 through a specific association of the SIR complex upstream of the promoter region. *THI4* was not identified from earlier ChIP-chip experiments as being bound by Sir2, Sir3, or Sir4, perhaps due to a combination of modest enrichment and the relatively low resolution of ChIP-chip probes at the time (31). However, the Sir proteins were shown in the same ChIP-chip study to associate with several genes other than the known heterochromatic regions. The mechanism of this unexpected SIR recruitment to specific genes other than the known heterochromatic regions remains unknown. Taken together, a picture emerges in which different functional classes of sirtuin-repressed genes utilize specific combinations of Hst1 and two of the other sirtuins (Sir2 and Hst2) to control transcription. More work is needed to determine whether Hst3 and Hst4 regulate specific gene transcription.

Interplay between thiamine and NAD$^+$. The finding that *THI* gene expression is repressed by the NAD$^+$-dependent sirtuin Hst1 is highly intriguing because of the recent discovery that NAD$^+$ can be utilized as a substrate for thiamine biosynthesis at the Thi4-catalyzed step to form the thiazole HET-P intermediate (12). PLP can be used as a pyrimidine source in the synthesis of thiamine, and several genes that function in the synthesis of PLP were also identified as being derepressed in the microarray experiment by reductions in NAD$^+$ concentration or increased NAM concentration. In rich medium with abundant thiamine and nicotinic acid, yeast cells are able to efficiently import these precursors of thiamine pyrophosphate and NAD$^+$, respectively, and the biosynthesis pathways are therefore repressed. However, under natural environmental conditions or in minimal medium with low thiamine and nicotinic acid levels, the cells respond by coordinately upregulating *de novo* NAD$^+$ biosynthesis genes with thiamine and PLP biosynthesis genes. Perhaps one of the reasons for the coregulation is that it ensures that the cells have sufficient quantities of NAD$^+$ and PLP for thiamine production during times of low nutrient exposure, although the need for proper coordination of other metabolic pathways dependent on these vitamins is also likely. In addition to NAD$^+$ and thiamine biosynthesis genes, the thiamine and NAD$^+$ transport genes are also upregulated in YPD medium when Hst1 or Sum1 is deleted. The combined increase in biosynthesis and transport likely leads to the increase in thiamine concentration we observe in the *npt1*Δ, *sum1*Δ, and *hst1*Δ mutants. These thiamine measurements were performed with cells grown in YPD medium. Since we were able to detect significant increases in cellular thiamine concentration in the mutants, this strongly suggests that keeping the thiamine biosynthesis genes in a fully repressed basal state via Hst1 is important for maintaining proper thiamine homeostasis.

Thi71 provides another interesting link between thiamine and NAD$^+$. Thi71 was initially characterized as a protein with similarity to the main thiamine transporter, Thi7, and was found to have relatively weak thiamine transport activity (16). More recently, it was identified as the high-affinity transporter that imports extracellular nicotinamide riboside into the cell, hence its new name of Nrt1 (5). Nrt1/Thi71 has the capacity to transport both nicotinamide riboside and thiamine, though it appears that nicotinamide riboside is its primary substrate. This direct role of Nrt1/Thi71 in nicotinamide riboside transport clearly places Nrt1/Thi71 in the category of proteins involved in producing NAD$^+$ that are regulated by Hst1. Deleting *SIR2* had only a very small effect on *NRT1*/*THI71* expression and had no effect on local H3/H4 acetylation upstream of the promoter, at least with the antibodies used in the ChIP assay. (Fig. 6B). Therefore, any small effect of *SIR2* on the expression of this gene is likely indirect, with Hst1 being responsible for the direct NAD$^+$-dependent histone deacetylation. For genes such as *THI4* and *THI13*, which are truly dedicated to thiamine biosynthesis, there appears to be more redundancy between Sir2 and Hst1 in specifically repressing their basal expression level. Together, the results from this study add NAD$^+$ metabolism and sirtuin biology into the complexity of thiamine homeostasis and gene regulation.

ACKNOWLEDGMENTS

We thank David Auble for critical reading of the manuscript and additional members of the Smith and Bekiranov laboratories for helpful suggestions and comments. Purified nicotinamide riboside was kindly provided by Charles Brenner (University of Iowa).

This work was funded by U.S. National Institutes of Health grant GM075240 to J. S. Smith. Support for J. M. McClure was also provided by NIH Training Grant GM008136.

We declare that we have no conflict of interest.

REFERENCES

1. **Anderson, R. M., K. J. Bitterman, J. G. Wood, O. Medvedik, H. Cohen, S. S. Lin, J. K. Manchester, J. I. Gordon, and D. A. Sinclair.** 2002. Manipulation of a nuclear NAD$^+$ salvage pathway delays aging without altering steady-state NAD$^+$ levels. J. Biol. Chem. **277:**18881–18890.
2. **Ausubel, F. M., R. Brent, R. E. Kingston, D. D. Moore, J. G. Seidman, J. A. Smith, and K. Struhl (ed.).** 2000. Current protocols in molecular biology, vol. 2. John Wiley & Sons, Inc., New York, NY.
3. **Bedalov, A., M. Hirao, J. Posakony, M. Nelson, and J. Simon.** 2003. NAD$^+$-dependent deacetylase Hst1p controls biosynthesis and cellular NAD$^+$ levels in *Saccharomyces cerevisiae*. Mol. Cell. Biol. **23:**7044–7054.
4. **Belenky, P., F. G. Racette, K. L. Bogan, J. M. McClure, J. S. Smith, and C. Brenner.** 2007. Nicotinamide riboside promotes Sir2 silencing and extends lifespan via Nrk and Urh1/Pnp1/Meu1 pathways to NAD$^+$. Cell **129:**473–484.
5. **Belenky, P. A., T. G. Moga, and C. Brenner.** 2008. *Saccharomyces cerevisiae YOR071C* encodes the high affinity nicotinamide riboside transporter Nrt1. J. Biol. Chem. **283:**8075–8079.
6. **Bieganowski, P., H. C. Pace, and C. Brenner.** 2003. Eukaryotic NAD$^+$ synthetase Qns1 contains an essential, obligate intramolecular thiol glutamine amidotransferase domain related to nitrilase. J. Biol. Chem. **278:**33049–33055.
7. **Bitterman, K. J., R. M. Anderson, H. Y. Cohen, M. Latorre-Esteves, and D. A. Sinclair.** 2002. Inhibition of silencing and accelerated aging by nicotinamide, a putative negative regulator of yeast sir2 and human SIRT1. J. Biol. Chem. **277:**45099–45107.
8. **Brachmann, C. B., J. M. Sherman, S. E. Devine, E. E. Cameron, L. Pillus, and J. D. Boeke.** 1995. The *SIR2* gene family, conserved from bacteria to humans, functions in silencing, cell cycle progression, and chromosome stability. Genes Dev. **9:**2888–2902.
9. **Buck, S. W., C. M. Gallo, and J. S. Smith.** 2004. Diversity in the Sir2 family of protein deacetylases. J. Leukoc. Biol. **75:**939–950.
10. **Buck, S. W., J. J. Sandmeier, and J. S. Smith.** 2002. RNA polymerase I propagates unidirectional spreading of rDNA silent chromatin. Cell **111:**1003–1014.
11. **Burke, D., D. Dawson, and T. Stearns.** 2000. Methods in yeast genetics. Cold Spring Harbor Laboratory Press, Cold Spring Harbor, NY.
12. **Chatterjee, A., C. T. Jurgenson, F. C. Schroeder, S. E. Ealick, and T. P. Begley.** 2007. Biosynthesis of thiamin thiazole in eukaryotes: conversion of NAD to an advanced intermediate. J. Am. Chem. Soc. **129:**2914–2922.
13. **Dietrich, F. S., S. Voegeli, S. Brachat, A. Lerch, K. Gates, S. Steiner, C. Mohr, R. Pohlmann, P. Luedi, S. Choi, R. A. Wing, A. Flavier, T. D. Gaffney, and P. Philippsen.** 2004. The *Ashbya gossypii* genome as a tool for mapping the ancient *Saccharomyces cerevisiae* genome. Science **304:**304–307.
14. **Edgar, R., M. Domrachev, and A. E. Lash.** 2002. Gene expression omnibus: NCBI gene expression and hybridization array data repository. Nucleic Acids Res. **30:**207–210.
15. **Eijkman, C.** 1990. Anti-neuritis vitamin and beriberi. Nobel prize paper. 1929. Ned Tijdschr Geneeskd **134:**1654–1657. (In Dutch.)
16. **Enjo, F., K. Nosaka, M. Ogata, A. Iwashima, and H. Nishimura.** 1997. Isolation and characterization of a thiamin transport gene, *THI10*, from *Saccharomyces cerevisiae*. J. Biol. Chem. **272:**19165–19170.
17. **Gallo, C. M., D. L. Smith, Jr., and J. S. Smith.** 2004. Nicotinamide clearance by Pnc1 directly regulates Sir2-mediated silencing and longevity. Mol. Cell. Biol. **24:**1301–1312.
18. **Gentleman, R., V. Carey, W. Huber, R. Irizarry, and S. Dudoit (ed.)** 2005. Bioinformatics and computational biology solutions using R and Bioconductor. Springer, New York, NY.
19. **Ghislain, M., E. Talla, and J. M. Francois.** 2002. Identification and functional analysis of the *Saccharomyces cerevisiae* nicotinamidase gene, *PNC1*. Yeast **19:**215–224.
20. **Halme, A., S. Bumgarner, C. Styles, and G. R. Fink.** 2004. Genetic and epigenetic regulation of the *FLO* gene family generates cell-surface variation in yeast. Cell **116:**405–415.
21. **Hickman, M. A., and L. N. Rusche.** 2007. Substitution as a mechanism for genetic robustness: the duplicated deacetylases Hst1p and Sir2p in *Saccharomyces cerevisiae*. PLoS Genet. **3:**e126.
22. **Hohmann, S., and P. A. Meacock.** 1998. Thiamin metabolism and thiamin diphosphate-dependent enzymes in the yeast *Saccharomyces cerevisiae*: genetic regulation. Biochim. Biophys. Acta **1385:**201–219.

23. **Imai, S.-i., C. M. Armstrong, M. Kaeberlein, and L. Guarente.** 2000. Transcriptional silencing and longevity protein Sir2 is an NAD-dependent histone deacetylase. Nature **403:**795–800.
24. **Kellis, M., B. W. Birren, and E. S. Lander.** 2004. Proof and evolutionary analysis of ancient genome duplication in the yeast *Saccharomyces cerevisiae*. Nature **428:**617–624.
25. **Kowalska, E., and A. Kozik.** 2008. The genes and enzymes involved in the biosynthesis of thiamin and thiamin diphosphate in yeasts. Cell. Mol. Biol. Lett. **13:**271–282.
26. **Kucharczyk, R., M. Zagulski, J. Rytka, and C. J. Herbert.** 1998. The yeast gene YJR025c encodes a 3-hydroxyanthranilic acid dioxygenase and is involved in nicotinic acid biosynthesis. FEBS Lett. **424:**127–130.
27. **Landry, J., J. T. Slama, and R. Sternglanz.** 2000. Role of NAD^+ in the deacetylase activity of the SIR2-like proteins. Biochem. Biophys. Res. Commun. **278:**685–690.
28. **Landry, J., A. Sutton, S. T. Tafrov, R. C. Heller, J. Stebbins, L. Pillus, and R. Sternglanz.** 2000. The silencing protein SIR2 and its homologs are NAD-dependent protein deacetylases. Proc. Natl. Acad. Sci. U. S. A. **97:**5807–5811.
29. **Langley, E., M. Pearson, M. Faretta, U. M. Bauer, R. A. Frye, S. Minucci, P. G. Pelicci, and T. Kouzarides.** 2002. Human SIR2 deacetylates p53 and antagonizes PML/p53-induced cellular senescence. EMBO J. **21:**2383–2396.
30. **Lee, S. E., F. Paques, J. Sylvan, and J. E. Haber.** 1999. Role of yeast *SIR* genes and mating type in directing DNA double-strand breaks to homologous and non-homologous repair paths. Curr. Biol. **9:**767–770.
31. **Lieb, J. D., X. Liu, D. Botstein, and P. O. Brown.** 2001. Promoter-specific binding of Rap1 revealed by genome-wide maps of protein-DNA association. Nat. Genet. **28:**327–334.
32. **Lin, S.-J., P.-A. Defossez, and L. Guarente.** 2000. Requirement of NAD and SIR2 for life-span extension by calorie restriction in *Saccharomyces cerevisiae*. Science **289:**2126–2128.
33. **Llorente, B., and B. Dujon.** 2000. Transcriptional regulation of the *Saccharomyces cerevisiae DAL5* gene family and identification of the high affinity nicotinic acid permease *TNA1* (*YGR260w*). FEBS Lett. **475:**237–241.
34. **Longtine, M. S., A. McKenzie III, D. J. Demarini, N. G. Shah, A. Wach, A. Brachat, P. Philippsen, and J. R. Pringle.** 1998. Additional modules for versatile and economical PCR-based gene deletion and modification in *Saccharomyces cerevisiae*. Yeast **14:**953–961.
35. **Loo, S., and J. Rine.** 1995. Silencing and heritable domains of gene expression. Annu. Rev. Cell Dev. Biol. **11:**519–548.
36. **Lorenz, M. C., R. S. Muir, E. Lim, J. McElver, S. C. Weber, and J. Heitman.** 1995. Gene disruption with PCR products in *Saccharomyces cerevisiae*. Gene **158:**113–117.
37. **Lu, J., and E. L. Frank.** 2008. Rapid HPLC measurement of thiamine and its phosphate esters in whole blood. Clin. Chem. **54:**901–906.
38. **Luo, J., A. Y. Nikolaev, S. Imai, D. Chen, F. Su, A. Shiloh, L. Guarente, and W. Gu.** 2001. Negative control of p53 by Sir2α promotes cell survival under stress. Cell **107:**137–148.
39. **McClure, J. M., C. M. Gallo, D. L. Smith, Jr., M. Matecic, R. D. Hontz, S. W. Buck, F. G. Racette, and J. S. Smith.** 2008. Pnc1p-mediated nicotinamide clearance modifies the epigenetic properties of rDNA silencing in *Saccharomyces cerevisiae*. Genetics **180:**797–810.
40. **McCord, R., M. Pierce, J. Xie, S. Wonkatal, C. Mickel, and A. K. Vershon.** 2003. Rfm1, a novel tethering factor required to recruit the Hst1 histone deacetylase for repression of middle sporulation genes. Mol. Cell. Biol. **23:**2009–2016.
41. **Mojzita, D., and S. Hohmann.** 2006. Pdc2 coordinates expression of the *THI* regulon in the yeast *Saccharomyces cerevisiae*. Mol. Genet. Genomics **276:**147–161.
42. **Nishimura, H., Y. Kawasaki, K. Nosaka, Y. Kaneko, and A. Iwashima.** 1991. A constitutive thiamine metabolism mutation, *thi80*, causing reduced thiamine pyrophosphokinase activity in *Saccharomyces cerevisiae*. J. Bacteriol. **173:**2716–2719.
43. **Nosaka, K.** 2006. Recent progress in understanding thiamin biosynthesis and its genetic regulation in *Saccharomyces cerevisiae*. Appl. Microbiol. Biotechnol. **72:**30–40.
44. **Nosaka, K., M. Onozuka, H. Konno, Y. Kawasaki, H. Nishimura, M. Sano, and K. Akaji.** 2005. Genetic regulation mediated by thiamin pyrophosphate-binding motif in *Saccharomyces cerevisiae*. Mol. Microbiol. **58:**467–479.
45. **Parra, M. A., D. Kerr, D. Fahy, D. J. Pouchnik, and J. J. Wyrick.** 2006. Deciphering the roles of the histone H2B N-terminal domain in genome-wide transcription. Mol. Cell. Biol. **26:**3842–3852.
46. **Parra, M. A., and J. J. Wyrick.** 2007. Regulation of gene transcription by the histone H2A N-terminal domain. Mol. Cell. Biol. **27:**7641–7648.
47. **Rajavel, M., D. Lalo, J. W. Gross, and C. Grubmeyer.** 1998. Conversion of a cosubstrate to an inhibitor: phosphorylation mutants of nicotinic acid phosphoribosyltransferase. Biochemistry **37:**4181–4188.
48. **Revollo, J. R., A. A. Grimm, and S. I. Imai.** 2004. The NAD biosynthesis pathway mediated by nicotinamide phosphoribosyltransferase regulates Sir2 activity in mammalian cells. J. Biol. Chem. **279:**50754–50763.
49. **Robert, F., D. K. Pokholok, N. M. Hannett, N. J. Rinaldi, M. Chandy, A. Rolfe, J. L. Workman, D. K. Gifford, and R. A. Young.** 2004. Global position and recruitment of HATs and HDACs in the yeast genome. Mol. Cell **16:**199–209.
50. **Robyr, D., Y. Suka, I. Xenarios, S. K. Kurdistani, A. Wang, N. Suka, and M. Grunstein.** 2002. Microarray deacetylation maps determine genome-wide functions for yeast histone deacetylases. Cell **109:**437–446.
51. **Sandmeier, J. J., I. Celic, J. D. Boeke, and J. S. Smith.** 2002. Telomeric and rDNA silencing in *Saccharomyces cerevisiae* are dependent on a nuclear NAD^+ salvage pathway. Genetics **160:**877–889.
52. **Sauve, A. A., I. Celic, J. Avalos, H. Deng, J. D. Boeke, and V. L. Schramm.** 2001. The chemistry of gene silencing: the mechanism of NAD^+-dependent deacetylation reactions. Biochemistry **40:**15456–15463.
53. **Smith, J. S., and J. D. Boeke.** 1997. An unusual form of transcriptional silencing in yeast ribosomal DNA. Genes Dev. **11:**241–254.
54. **Smith, J. S., C. B. Brachmann, I. Celic, M. A. Kenna, S. Muhammad, V. J. Starai, J. L. Avalos, J. C. Escalante-Semerena, C. Grubmeyer, C. Wolberger, and J. D. Boeke.** 2000. A phylogenetically conserved NAD^+-dependent protein deacetylase activity in the Sir2 protein family. Proc. Natl. Acad. Sci. U. S. A. **97:**6658–6663.
55. **Suka, N., Y. Suka, A. A. Carmen, J. Wu, and M. Grunstein.** 2001. Highly specific antibodies determine histone acetylation site usage in yeast heterochromatin and euchromatin. Mol. Cell **8:**473–479.
56. **Sutton, A., R. C. Heller, J. Landry, J. S. Choy, A. Sirko, and R. Sternglanz.** 2001. A novel form of transcriptional silencing by Sum1-1 requires Hst1 and the origin recognition complex. Mol. Cell. Biol. **21:**3514–3522.
57. **Tanny, J. C., and D. Moazed.** 2001. Coupling of histone deacetylation to NAD breakdown by the yeast silencing protein Sir2: evidence for acetyl transfer from substrate to an NAD breakdown product. Proc. Natl. Acad. Sci. U. S. A. **98:**415–420.
58. **Vaziri, H., S. K. Dessain, E. Ng Eaton, S. I. Imai, R. A. Frye, T. K. Pandita, L. Guarente, and R. A. Weinberg.** 2001. hSIR2(SIRT1) functions as an NAD-dependent p53 deacetylase. Cell **107:**149–159.
59. **Wolfe, K. H., and D. C. Shields.** 1997. Molecular evidence for an ancient duplication of the entire yeast genome. Nature **387:**708–713.
60. **Xie, J., M. Pierce, V. Gailus-Durner, M. Wagner, E. Winter, and A. K. Vershon.** 1999. Sum1 and Hst1 repress middle sporulation-specific gene expression during mitosis in *Saccharomyces cerevisiae*. EMBO J. **18:**6448–6454.
61. **Yeung, F., J. E. Hoberg, C. S. Ramsey, M. D. Keller, D. R. Jones, R. A. Frye, and M. W. Mayo.** 2004. Modulation of NF-κB-dependent transcription and cell survival by the SIRT1 deacetylase. EMBO J. **23:**2369–2380.